# Full Size Frequency Converter for Fast Francis Pump-Turbine Operating Mode Transition

**Christophe NICOLET**   Power Vision Engineering Sàrl, Ecublens, Switzerland

**Olivier BRAUN**   ANDRITZ HYDRO SA, Vevey, Switzerland

**Nicolas RUCHONNET**   ANDRITZ HYDRO SA, Vevey, Switzerland

**Antoine BEGUIN**   Power Vision Engineering Sàrl, Ecublens, Switzerland

**Johann HELL**   ANDRITZ HYDRO GmbH, Vienna, Austria

**François AVELLAN**   EPFL Laboratory for Hydraulic Machines, Lausanne, Switzerland

## Abstract

This paper explore the additional services that Full Size Frequency Converter, FSFC, solution can provide for the case of an existing pumped storage power plant of 2x210 MW which conversion from fixed speed to variable speed is investigated with a focus on fast mode transition. First, reduced scale model tests experiments of fast transition of Francis pump-turbine which have been performed at the ANDRITZ HYDRO Hydraulic Laboratory in Linz Austria are presented. The tests consists of linear speed transition from pump to turbine and vice versa performed with constant guide vane opening. Main results of head and discharge variations induced by the operating mode transition achieved with different transition time are presented. Then, the existing pumped storage power plant with pump-turbine quasi homologous to the reduced scale model is modelled using the simulation software SIMSEN considering the reservoirs, penstocks, the two Francis pump-turbines, the two downstream surge tanks, and the tailrace tunnel. For the electrical part, an FSFC configuration is considered with two different modelling approaches: (i) a detailed electrical model and (ii) a very simplified electromechanical model. The transitions from turbine to pump and vice versa are simulated, and similarities between prototype simulation results and reduced scale model experiments are highlighted. Finally, the plausibility of the fast transition on the prototype is evaluated by means of numerical simulation and is discussed according to extreme values obtained for different transition sequences.

## 1. Introduction

The integration of the constantly growing capacity of New Renewable Energies, NRE, mainly composed by wind and solar energies, is a challenging task as far as the power network stability is concerned, due to the intermittent nature of these energy sources, [30], [17]. Beside storage and substitution production capabilities, pumped storage power plants can significantly contribute to improve the stability of power network due to their production flexibility, fast response time and large energy storage capability, [5], [14]. Variable speed motor-generator solutions enable to provide a variety of new control services to the electrical grid to be carefully considered. In particular, solution based on synchronous motor-generator with Full Size Frequency Converter, FSFC, offer the possibility to achieve turbine to pump fast transition mode and vice versa. The feasibility of this new ancillary service was deeply investigated in the framework of the HYPERBOLE European Research Project, [32] by means of reduced scale model tests and numerical simulation, [23], [29]. This paper presents experimental and numerical results of fast mode transition from pump to turbine and vice versa performed on a reduced scale model tests as well as simulation results performed for an existing 2x210 MW pumped storage power plant equipped with a pump-turbine homologous to the reduced scale model, where conversion from fixed speed to FSFC variable speed solution is assumed. The plausibility of fast transition mode is investigated by means of full hydroelectric power plant simulation including both hydraulic system as well as electrical installations. For optimisation

1

purpose, a simplified simulation model of the FSFC solution was setup and dully validated against detailed simulation model.

## 2. Concepts and advantages of fast transitions with FSFC

### 2.1. Variable speed technologies

Despite higher investment cost related to additional equipment and associated civil work, variable speed technologies applied to pumped storage power plants offer variety of advantages such as [6], [11], [12], [13], [15], [16], [20], [21], [22], [26], [27], [28]:

- Active power control in pumping mode;

- Fast active power injection/absorption in pump and turbine mode thanks to "Flywheel" effect;

- Extended operating range in turbine and pumping mode;

- Higher efficiency in turbine mode;

- Pump start-up without supplementary equipment;

- Suitability for large head variations in pump mode;

- Reactive power control with Static Var Compensator even when the unit is at standstill.

Nowadays, two different variable speed technologies are available for pumped storage power plants, see Figure 1:
- **Doubly fed induction machines (DFIM):** AC current is fed to the rotor of asynchronous motor-generator using frequency converter enabling a unit rotational speed variation of typically +/- 10% resulting in a frequency converter nominal power of about 10% of the motor-generator power;

- **Synchronous machines equipped with Full Size Frequency Converter (FSFC):** The stator of conventional synchronous machine is connected to the power network through a frequency converter which nominal power is 100% of the motor-generator power, but offering a full flexibility of rotational speed range of the unit.
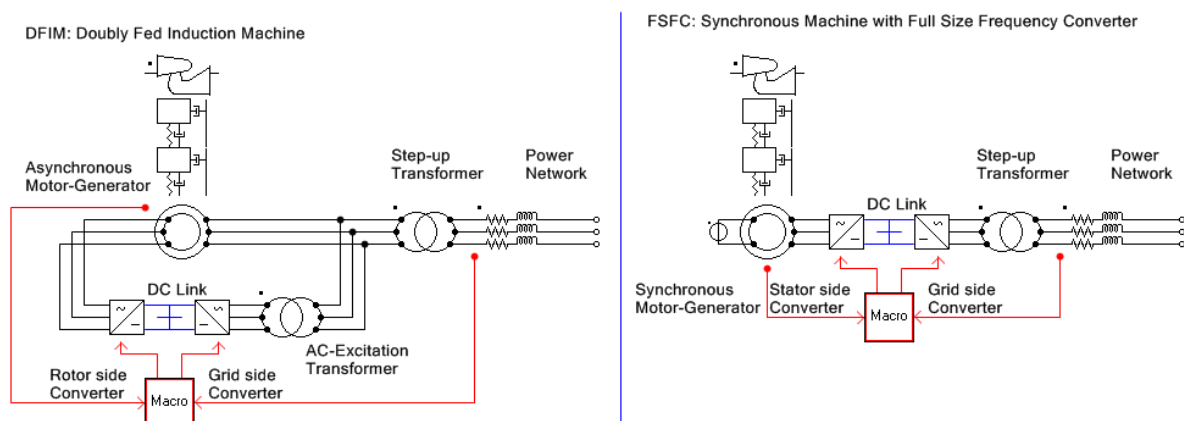


**Figure 1** DFIM and FSFC electromechanical configurations.

The selection of the most appropriate technology for a given pumped storage power plant is a complex process which should take into account aspects related to efficiency, operating range, excavation volumes and related civil engineering work, maintenance and equipment lifetime, and the expected ancillary services. Hildinger and Kodding [7] provided a detailed comparison of the two variable speed technologies also pointing out the technico-economical threshold between the DFIM and the FSFC solution currently set around 100 MW; FSFC being the most cost-effective solution for the lowest power and the DFIM being more cost effective solution for the higher power ratings.

Nevertheless, constant development in power electronics enable to expect to consider FSFC solution for higher power levels [2]. When both technologies are compared, the following aspects must be considered [7], [8], [9], [25]:

- Investment cost of FSFC is higher than for DFIM as the frequency converter power rating corresponds to 100% of the nominal unit power for FSFC while it corresponds only to the slip power for DFIM which is about 10% of the power rating for 10% speed variation, and also because higher excavation civil work is required due to the larger size of the frequency converter;

- The FSFC features a lower global efficiency than DFIM due to the losses of the frequency converter sized for the full rated power;

- The FSFC solution is based on fully proven synchronous motor-generator technology while the DFIM technology leads to complex AC rotor;

- The FSFC offers the maximum flexibility in speed range;

- The FSFC enable very fast start-up time and thus also very fast transition mode from pump to turbine and vice versa as no synchronization time is required and because almost nominal torque is available from standstill enabling direct pump start-up in water which is not possible with DFIM that requires first dewatering the unit.

Moreover, it could be noticed that the conversion of an existing fixed speed pump-turbine unit to variable speed could be achieved more easily when FSFC solution is considered, as it was the case for one unit of 100 MW at Grimsel II power plant in Switzerland, [25], as compared to the conversion from fixed speed to DFIM solution, [1].

### 2.2. Concept of Fast transitions

The ability of FSFC solution to control the rotational speed of the pump-turbine unit continuously over the whole rotational speed range from pump to turbine, and the capability to supply almost the nominal torque at zero speed, makes it possible to perform a direct transition from pump to turbine, and more challenging, is the direct transition from turbine to pump in a very short time without need for transition at standstill, see Figure 2, [8], [7]. Indeed, if conventional fixed speed pump-turbines as well as DFIM variable speed solutions would be capable to perform a fast transition from pump to turbine using a special procedure with transition without stop at standstill, the opposite transition requires a stop at zero speed to allow for dewatering the pump for start-up purpose. Therefore, for fixed speed and DFIM applications, the transition time from turbine to pump is not less than 240 s, [5], while it could be brought down to about 40 s using FSFC converter, [8], corresponding to a similar transition time of ternary units using hydraulic torque converters [5]. For both technical solutions, the limiting factor is more the hydraulic transients than the unit capabilities.
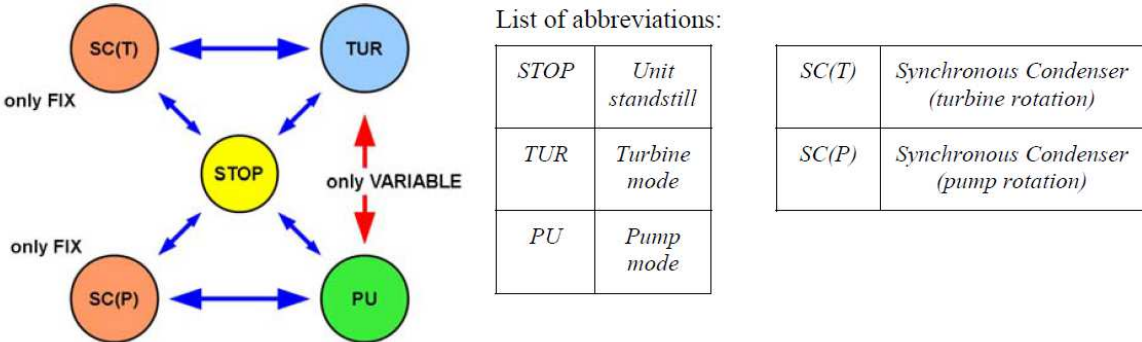


List of abbreviations:

| STOP | Unit standstill |
|---|---|
| TUR | Turbine mode |
| PU | Pump mode |

| SC(T) | Synchronous Condenser (turbine rotation) |
|---|---|
| SC(P) | Synchronous Condenser (pump rotation) |

**Figure 2** Operating mode of a pump-turbine unit [8].

## 3. Reduced scale model tests and simulations

The feasibility of fast mode transition from pump to turbine and vice versa is investigated first at the reduced model scale by means of both experimental and numerical approach enabling a comprehensive survey of the dynamic behavior of the pump-turbine unit and its interaction with the related hydraulic circuit. Then, numerical investigation is performed at the prototype scale for an existing 2x210 MW pumped-storage power plant which Francis pump-turbine is homologous to the reduced scale model pump-turbine to allow for transposition consideration. Indeed, Figure 3 presents the reduced scale model of the pump-turbine installed at the ANDRITZ Hydro Hydraulic Laboratory in Linz, Austria, as well as the corresponding prototype pump-turbine unit layout both having the same specific speed of $N_{QE}$=0.17 ($n_{SQ}$=207), the same blade number and main dimensions, and thus they are quasi homologous.
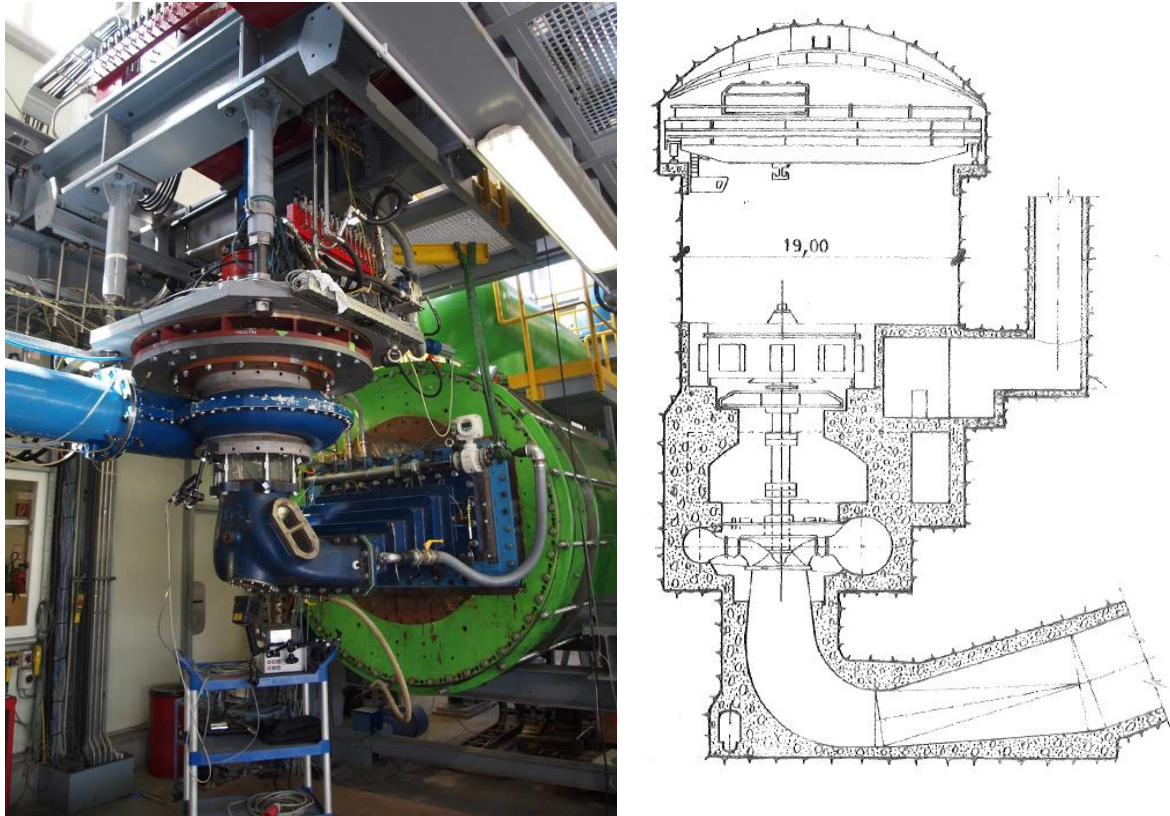


**Figure 3** Reduced scale model installed on ANDRITZ Hydro test rig in Linz (left) and corresponding homologous prototype layout (right) pump-turbine unit test case.

### 3.1. Test rig facility and fast transition test

Measurement of transitions from pump to turbine and vice versa performed on the pump-turbine reduced scale model at the ANDRITZ Hydro laboratory in Linz, Austria, used a dedicated test rig configuration, setup specifically for the HYPERBOLE Research Project, in order to perform the full transition with realistic flow conditions. The pump-turbine reduced scale model is mounted in parallel with a pump and a diaphragm made of a perforated plate, see Figure 4. The head losses through the diaphragm, ΔH, is proportional to the discharge power two, as follows:

$$\Delta H = k_r \cdot Q^2 = \frac{K_d}{2 \cdot g \cdot A_{ref}^2} Q^2 \qquad (1)$$

Where:

$K_d$: Singular head loss coefficient [-]
$A_{ref}$: Reference cross section area [m$^2$]
$k_r$: Head loss factor [s$^2$/m$^5$]

4

In pump mode, the discharge of both pump and pump-turbine flows through the diaphragm. In turbine mode, part of pump discharge flows through the pump-turbine, the other part through the diaphragm, see Figure 5. The head is maintained constant by varying the pump rotating speed. During transitions, linear speed ramps are imposed to both the pump-turbine and the pump using variable speed electric motor-generator which drive was adapted for the purpose of transition tests, see Figure 6. With this alternative test rig configuration, the transition as seen from the pump-turbine is close to the transition at prototype scale. The head variation is mainly driven by the fluid acceleration within the turbine branch of the circuit.

In addition to the standard model test instrumentation, dynamic pressure transducers are installed in the rotating and stationary parts of the turbine. Strain gauges are installed on guide vanes stems and turbine shaft for torque measurement. A dynamic flow meter is used to record the discharge variation. Measurements have been performed at constant guide vane opening for various transition time, guide vane opening, cavitation level and head. More details regarding the experimental setup and results can be found in [23].

The fast transition tests have been performed for the following guide vanes and transition times:
- Guide vanes openings: 5°, 15° and 25° (respectively 0.125, 0.375 and 0.625 pu);
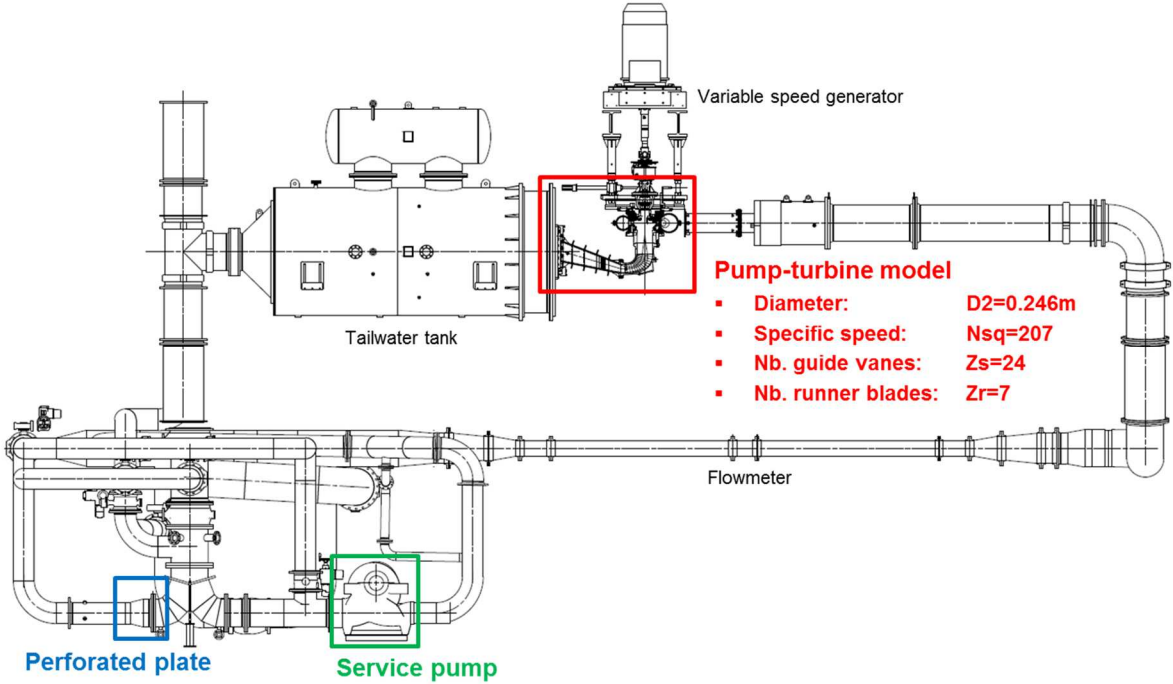
- Transition time: 4 s, 8 s, 12 s, 20 s.



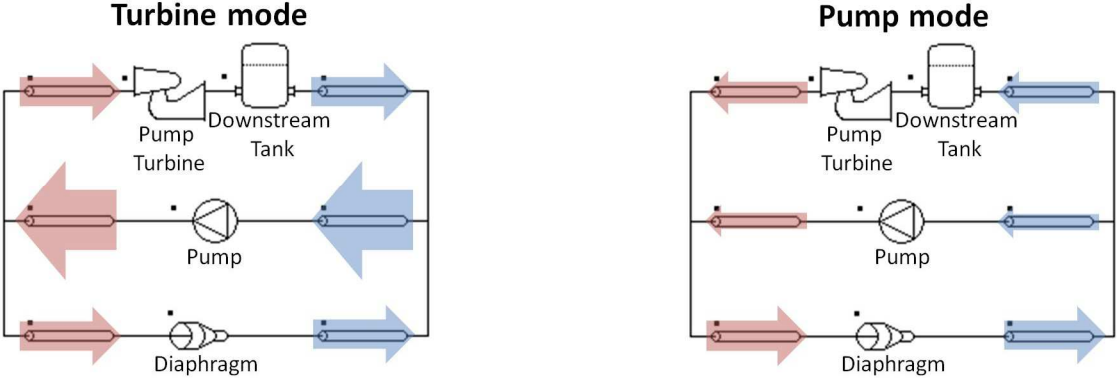**Figure 4** Side view of the ANDRITZ Hydro test rig facility in Linz, Austria.



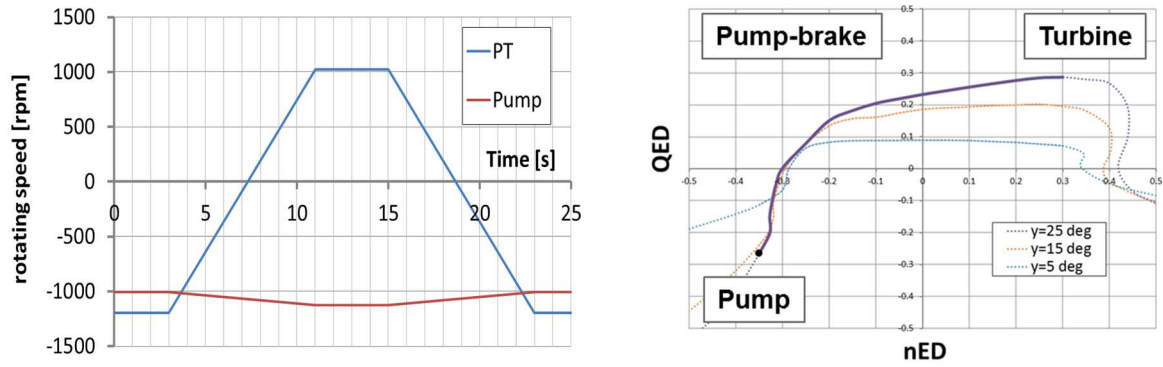**Figure 5** Test rig configuration for pump-turbine transition.

**Figure 6** Time evolution of the pump-turbine (PT) and feed pump (Pump) rotational speed imposed during pump-turbine fast transition experimental tests (left) and resulting pump-turbine transient operating point for 25° guide vane opening (right).

### 3.1. Measurements results for fast transitions

As an example, the time evolution of guide vane torque is presented in Figure 7 for a transition from pump to turbine (from 3s to 11s) and back from turbine to pump (from 15s to 23s). During the transitions, large amplitude of torque fluctuation is observed. Maximum amplitude is reached in pump-break mode and the transition from turbine to pump leads to higher amplitudes than the transition from pump to turbine. Those measurements are used to assess the mechanical loading of the pump-turbine components during transition and also to validate transient CFD simulations, see [29] for more details on transient CFD simulations.
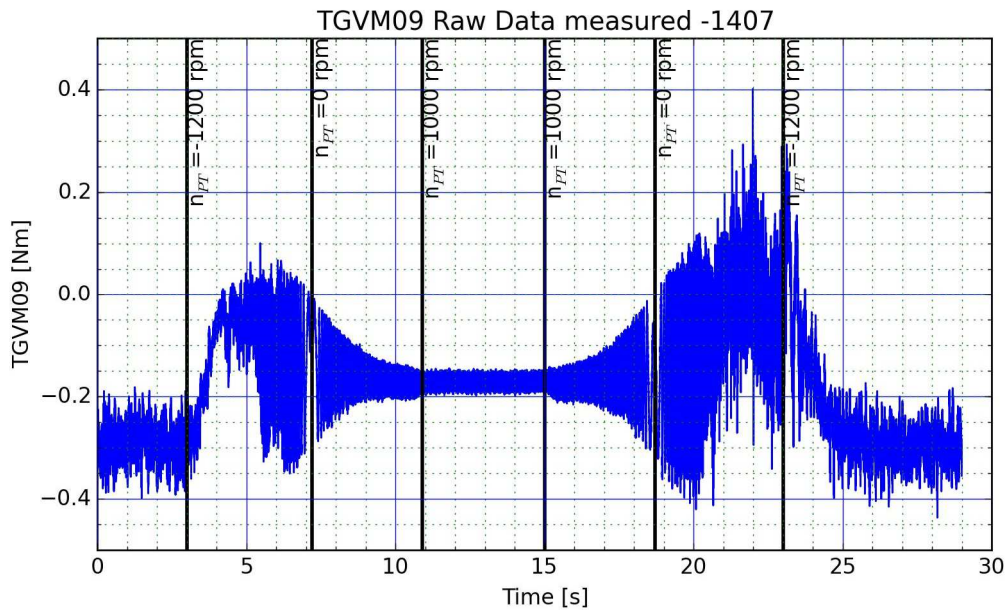


**Figure 7** Time evolution of guide vane torque.

### 3.1. Comparison between 1D simulations and measurements

A 1D model of the test rig has been setup using the SIMSEN simulation software developed by the Ecole polytechnique fédérale de Lausanne, EPFL, see [18], [19], [24]. The model includes the pipes dimensions of the entire test rig; the downstream reservoir; the pump and pump-turbine characteristics. Due to the complexity of the circuit, the head losses are calibrated based on the measurement results. Three transitions from pump to turbine and return are simulated and compared with test rig measurements. Transition starts at t=3s, the pump-turbine rotating speed is varied linearly in 4s, 8s and 12s respectively. Once in turbine mode, the speed is kept constant during 4s before returning to pump mode with the same transition time. The resulting time evolutions of head and discharge are in good agreement with the measurements, see Figure 8.
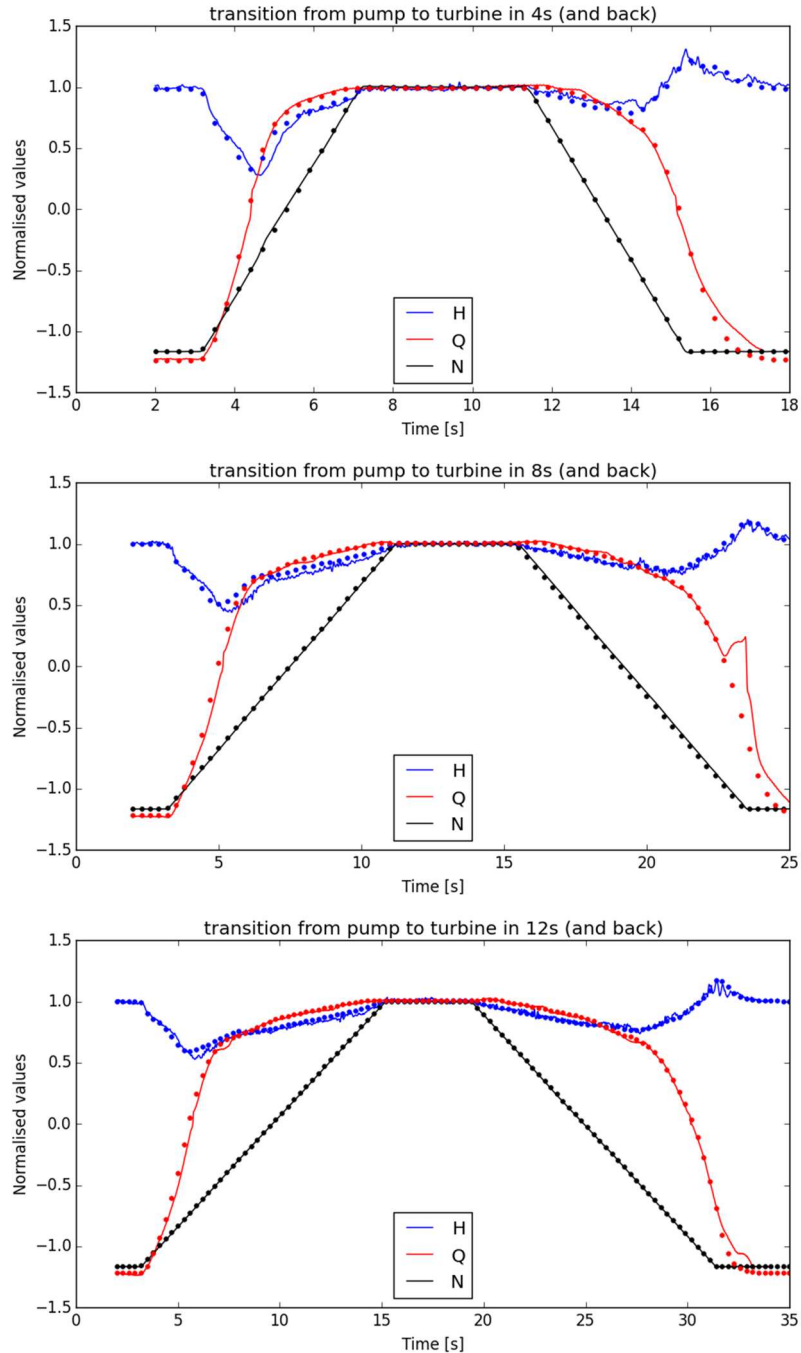
6

**Figure 8** Time evolution of normalized head, discharge and rotating speed during transition from pump to turbine and back to pump, comparison between measurement (line) and simulation (dots) for 4s, 8s and 12s transition time.

The signals are normalized with the reference value in turbine mode: reference head, Href=12mWC; reference discharge, Qref=0.128 m³/s, reference PT rotating speed, Nref=794 rpm. The measurements are indicated with a continuous line, the simulation is indicated with dots. The small deviations observed in the simulations for the head (blue) are probably due to the simplification made during the modeling of the piping system. The inaccurate estimation of water inertia leads to head deviation during transitions. The significant discrepancy in discharge (red) during the return from turbine to pump is due to the passage of air bubble in the flowmeter leading to error in the measurement. This comparison demonstrates the suitability of 1D model to predict the dynamic behavior of prototype during transition from turbine to pump and vice versa.

## 4. Prototype scale simulations

### 4.1. Prototype test case

Numerical simulation have been carried out in order to assess the feasibility of fast transition from pump to turbine mode of reversible Francis pump-turbine at the prototype scale, for an existing pumped storage power plant equipped with a Francis pump-turbine quasi homologous to the one considered for the reduced scale model tests, see Figure 3. Figure 9 presents the SIMSEN simulation model of the existing 2x210 MW pumped storage power plant considered for the investigations at the prototype scale which key characteristics are summarized in Table 1. The power plant includes the following components:

- An upper reservoir with constant water level;
- Two sub-horizontal intake pipes;
- The upstream gates;
- The two vertical circular pressure shafts;
- The two reversible Francis pump-turbines of 210 MW, to the rotating inertia of the turbine and of the motor-generator rotor;
- The draft tube and units downstream pipes;
- The two downstream surge tanks which are linked together in the lower part;
- The downstream junction and tailrace tunnel;
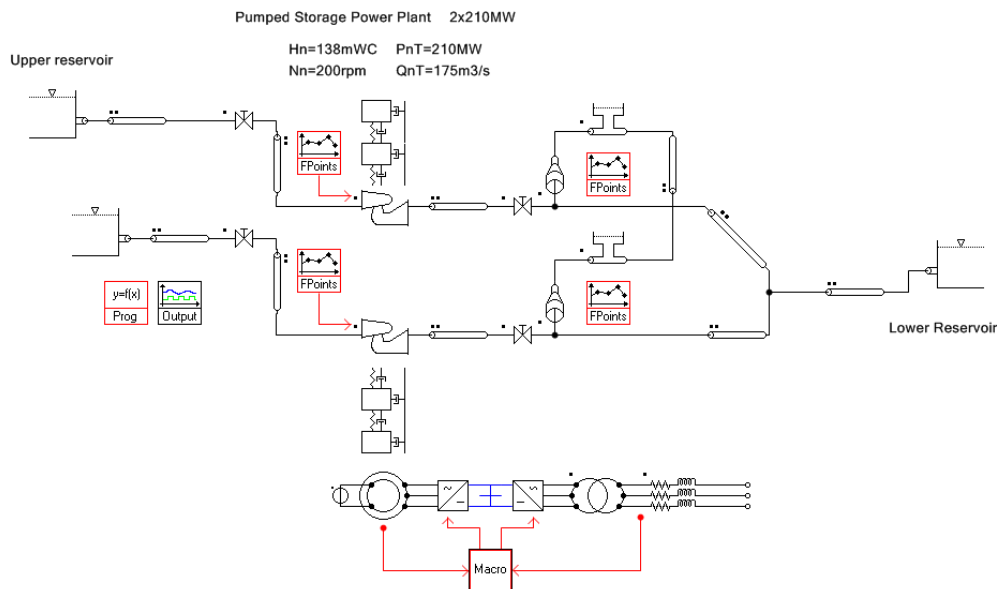- The lower reservoir with constant water level.



**Figure 9** SIMSEN model of the pumped storage power plant test case of 2 x 210 MW.

**Table 1** Pumped-storage power plant characteristics.

| Francis pump-turbine: | |
|---|---|
| Nominal rotational speed | 200 rpm |
| Turbine nominal power | 210 MW |
| Turbine nominal discharge | 175.1 m$^3$/s |
| Turbine nominal net head | 133.5 mWC |
| Turbine nominal torque | 9.74 MNm |
| Low pressure side diameter | 3.86 m |
| Total unit inertia including generator and turbine (J=MR$^2$) | 4106 t*m$^2$ |
| Mechanical time constant ($\tau_m = J_{tot} \cdot \omega_n^2 / P_n$ ) | 8.6 s |
| Synchronous motor-generator: | |
| Network frequency | 50 Hz |
| Apparent power | 210 MVA |
| Number of pair poles | 15 |
| Terminal/grid voltage | 15 kV / 400 kV |

### 4.1. Prototype SIMSEN modeling

#### 4.1.1.Hydraulic modelling

The SIMSEN hydraulic model, see Figure 9, includes all hydraulic components of the pumped storage power plant and takes into account [18], [19], [31]:

- Water hammer phenomena in piping systems (pipe head losses, water inertia and pipe elastic behaviour (fluid compressibility and wall deformation));

- The 4 quadrants transient behaviour of the pump-turbine, see Figure 10, including so-called S-shape unstable characteristics corresponding to the one considered for the reduced scale model tests, and the link with rotating inertias;

- The surge tank mass oscillations phenomena between the lower surge tanks and the lower reservoir taking into account variable cross section area of the surge tanks and asymmetric head losses at the inlet of the surge tank;

- The generating unit rotating train torsion dynamics with turbine and motor-generator rotor rotating inertia linked through coupling shaft with given torsional stiffness corresponding to the first natural torsional frequency of the unit.
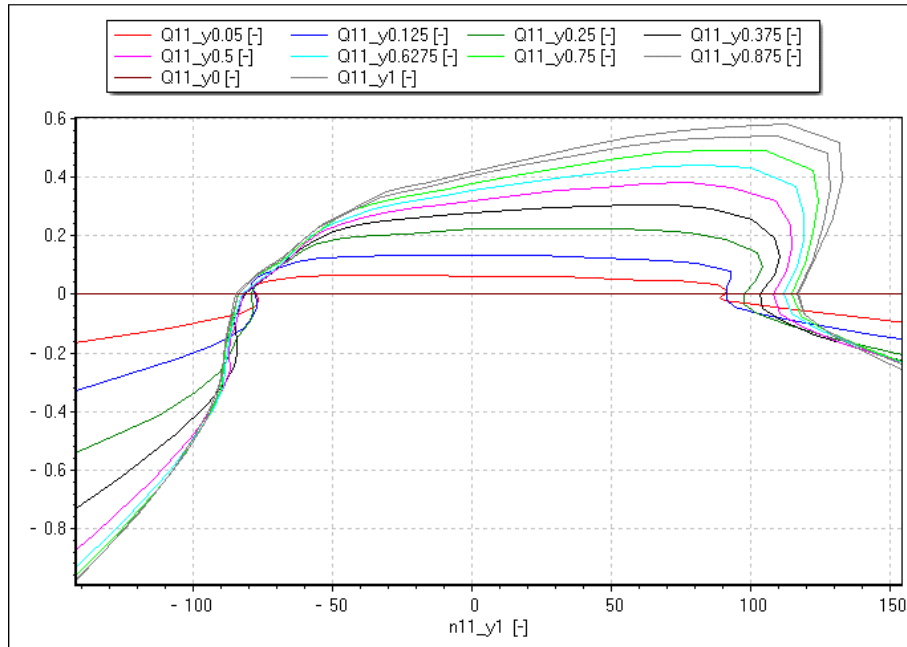


**Figure 10** Four quadrants Francis pump-turbine characteristics Q11=Q11(N11) considered in the SIMSEN model of the pumped storage power plant.

The numerical simulations are performed assuming that one of the unit is converted from fixed speed synchronous motor-generator to variable speed unit by the introduction of a Full Size Frequency Converter, FSFC, between the synchronous motor-generator and the step up transformer, see Figure 9. The hydromechanical model of the power plant assumed an ideal FSFC with synchronous motor-generator set enabling to achieve every fast linear transition from pump to turbine and vice versa. Therefore, the dynamic behavior of the motor-generator was first neglected, and the rotational speed of the pump-turbine unit was directly imposed to the unit with linear time evolution. Nevertheless, in order to assess the feasibility of the fast transitions, the electromechanical torque of the motor-generator was estimated using the angular momentum balance of the unit rotating masses expressed as follows:

$$J_{tot}\frac{d\omega}{dt}=T_{PT}+T_{MG} \qquad (2)$$

Where:

$J_{tot}$:     Total rotating inertia including motor-generator and turbine inertia [kg·m²]
$T_{PT}$:     Pump-turbine mechanical torque [Nm]
$T_{MG}$:     Motor-generator electromagnetic torque [Nm]
$\omega$:     Rotating pulsation [rd/s]

The motor-generator torque necessary to achieve a given rotational speed transition can be derived from equation (2) as follows:

$$T_{MG} = J_{tot}\frac{d\omega}{dt} - T_{PT} \tag{3}$$

While the corresponding active power can be calculated as follows:

$$P_{MG} = T_{MG} \cdot \omega \tag{4}$$

The rotational speed being imposed *a priori*, it enables to estimate the motor-generator transient electromagnetic torque as well as the corresponding power during the fast transitions with equations (3) and (4), to be compared with the unit nominal power and torque to evaluate the feasibility of the transition from the motor-generator perspective.

### 4.1.1. Detailed electrical modelling

In order to validate the simplified model of the motor-generator using equations (3) and (4), a fully detailed SIMSEN simulation model of the FSFC set was setup and simulation results have been compared with the simplified model. The SIMSEN model of the FSFC variable speed consists in the following elements: a synchronous machine, the machine side and grid side converters, the unit step-up transformer, a connection to the grid with a given finite short-circuit power and the unit rotating inertia. Table 1 provides the nominal values of the synchronous machine. The model of the synchronous machine is of high order and takes into account the excitation currents and damper currents, see [3], [4] [10]. Figure 11 presents the SIMSEN model of a FSFC variable speed pumped storage power plant.
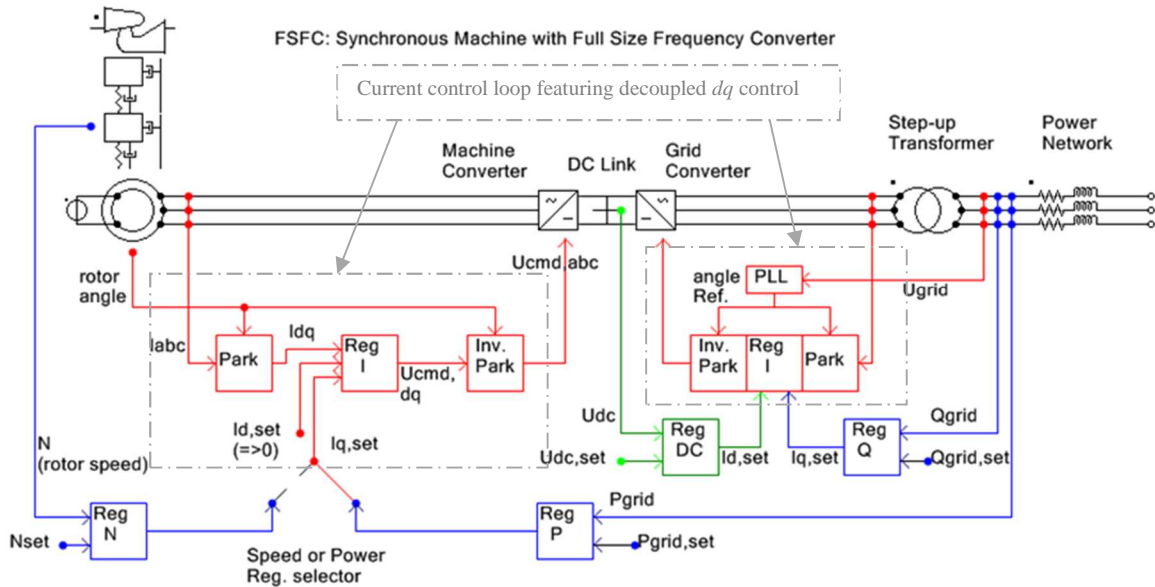


**Figure 11** SIMSEN model of power plant for the FSFC solution.

The key point in the detailed model is the control of the converters, on the machine side and on the grid side. The machine side converter operates either as a speed controller or as an active power controller, depending on the overall control strategy. It can operate in both modes because the underlying quantity that is controlled is the electro-magnetic torque. If the machine side converter controls the active power at the stator, the speed of the mechanical shaft is then maintained at a desired

10

set point by the turbine's governor. In turbine mode, the machine side converter is in active power mode, while the speed control mode is used for turbine to pump transition or vice versa.

The grid side converter operates as reactive power controller in order to offer voltage support to the grid. Besides, it ensures the transfer of active power from the machine side converter to the grid. This transfer of active power from stator to grid is ensured by the control of DC link voltage.

The basic inner control loop of the machine side converter is to control the stator currents of the electrical machine. The current control strategy choses an angular reference that is locked with rotor direct axis $d$. In this case, the quadrature component ($I_q$) of stator current is then proportional to the electro-magnetic torque (hence also active power) while the direct component ($I_d$) can influence the reactive power flow between stator and converter. As the study of reactive power flow at stator is not the focus in this project, the strategy is to set $I_d$=0, which corresponds to a maximum torque for a given stator current (neglecting the torque due to anisotropy of rotor). The current controller uses a decouple d-q architecture which allows to independently control direct and quadrature components of stator current.

### 4.2. Transposition from model to prototype

The dimension ratio between the Prototype (P) and reduced scale model (M) of the pump-turbine is given by the ratio between the reference diameter (low pressure side) of both runners and for the present test case is equal to:

$$\frac{D^P}{D^M} = \frac{3.86}{0.244} = 15.82$$

The Froude similitude has been considered to transpose the transition time from reduced scale model to the prototype scale, by expressing the reference velocity as function of the unit net head H, and then expressing the head H as function of the runner peripheral velocity $U = \omega \cdot R$ with $H = U^2/(2 \cdot g)$ as follows:

$$Fr = \frac{C_{ref}}{\sqrt{g \cdot D_{ref}}} = \sqrt{\frac{g \cdot H}{g \cdot D_{ref}}} = \sqrt{\frac{U^2}{2 \cdot g \cdot D_{ref}}} = \frac{\omega}{2}\sqrt{\frac{D_{ref}}{2 \cdot g}} \qquad (5)$$

From equation (5), the time ratio between model and prototype can expressed as follows:

$$\left(\frac{\omega^P}{\omega^M}\right)^2 = \frac{D^M}{D^P} \quad \rightarrow \quad \left(\frac{T^P}{T^M}\right)^2 = \frac{D^P}{D^M} \qquad (6)$$

According to the dimension ratio of $D^P/D^M = 15.82$ between the prototype and the model, the transition time ratio is given equal to:

$$\frac{T^P}{T^M} = \sqrt{\frac{D^P}{D^M}} = 3.98 \cong 4$$

According to the above transposition, the transition time considered during reduced scale model tests leads to the following transition time at the prototype scale:

- $T^M = 4s \rightarrow T^P = 4 \cdot 4s = 16s$

- $T^M = 8s \rightarrow T^P = 4 \cdot 8s = 32s$

- $T^M = 12s \rightarrow T^P = 4 \cdot 12s = 48s$

- $T^M = 20s \rightarrow T^P = 4 \cdot 20s = 80s$

### 4.3. Transposed fast transitions at Prototype scale for Y=15°

The numerical simulation of the fast transition from pump to turbine mode and vice versa is simulated at the prototype scale with transition time of 32s from pump nominal rotational speed N=-200 rpm to the turbine nominal rotational speed N=+200 rpm, to compare with the reduced scale model tests results. The transition time at the prototype scale of $T^P = 32s$ corresponds to $T^M = 8s$ at the reduced model scale. For the transition, constant guide vane of Y=15° (y=0.375 pu) is considered. Figure 12 presents the time evolution of the dimensionless characteristic quantities of the Prototype pump-turbine resulting from the fast transition, to be compared with the simulation and measurement results at the reduced scale of Figure 8 (middle). It could be highlighted that despite completely different hydraulic circuits between model and prototype, the qualitative evolution of the dimensionless net head $h$ and discharge $q$ shows remarkable similarities with sudden and sharp net head drop during the pump to turbine transition and a net head rise during the turbine to pump transition. These net head variations results respectively from the discharge acceleration and deceleration. But of course, direct transposition of the transient behavior of the pump-turbine unit from reduced scale model test to prototype is not possible since the related hydraulic systems are not in similitude. And hence transposition can only be investigated by means of numerical simulation. Figure 13 presents the time evolution of the pump-turbine spiral case and draft tube pressure resulting from the fast transitions which remains within acceptable values. Figure 14 presents the time evolution of the transient operating point of the prototype pump-turbine during the fast transitions from pump to turbine and return. Finally, Figure 15 presents the time evolution of the electromagnetic torque and the related active power calculated according to equations (3) and (4). As expected, the transition from pump to turbine does not lead to large values of the electromagnetic quantities as the transition induces a discharge reversal supported by the gravity forces. However, during the transition from turbine to pump, extreme values of electromagnetic torque and active power are reached due to discharge reversal against gravity forces leading to 1.7 times the nominal torque at t=115s and a maximum active power of 240 MW at t=132s representing 114% of the nominal power of the unit. The maximum torque occurs during the zero rotational speed cross over, while the maximum active power occurs at the end of the fast transition, emphasizing the importance of monitoring both quantities during the transition and not only restricting the analysis to active power.
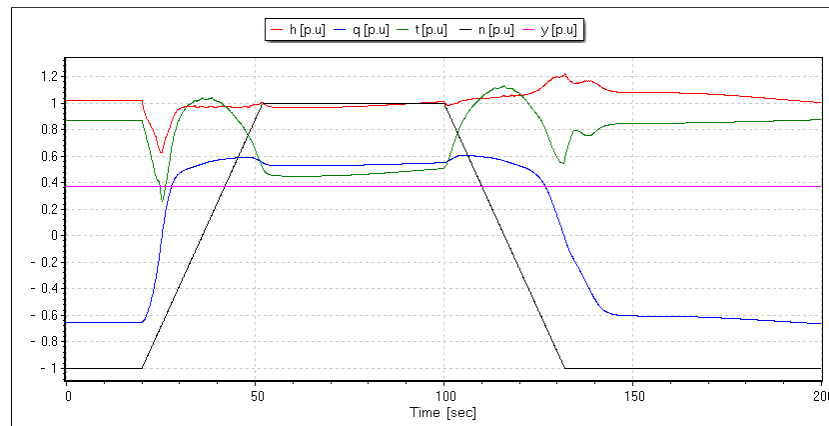


**Figure 12** Simulation results of the fast transition from pump to turbine and vice-versa at the Prototype scale considering Y=15° (y=0.375 pu) and 32s of transition time corresponding to 8s transition at the reduced scale model.
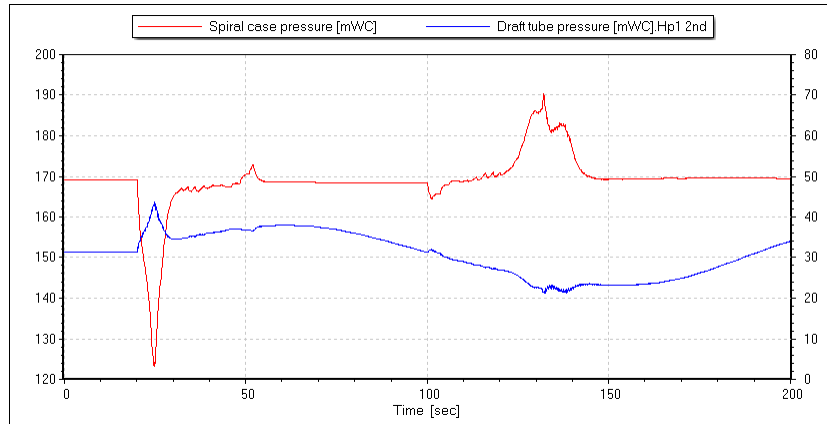
**Figure 13** Time evolution of the spiral case and draft tube pressures of the pump turbine simulation results of the fast transition from pump to turbine and vice-versa at the Prototype scale considering Y=15° (y=0.375 pu) and 32s of transition time corresponding to 8s transition at the reduced scale model.
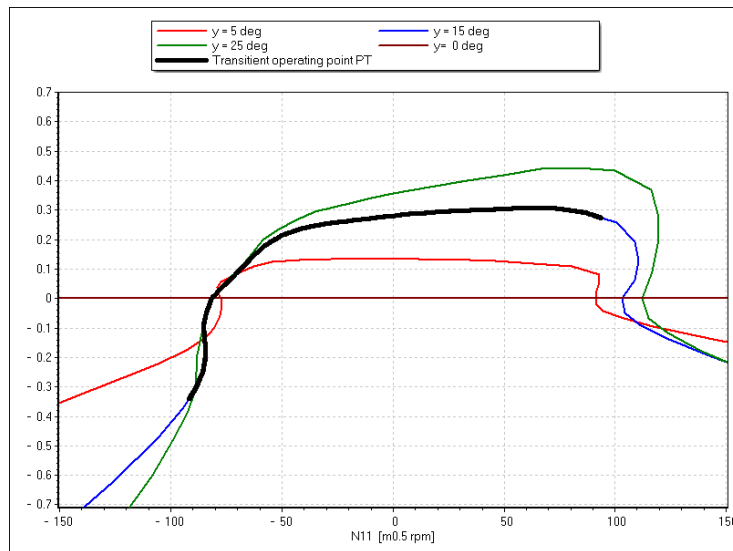


**Figure 14** Transient operating point of the pump turbine during the fast transition from pump to turbine and vice-versa at the Prototype scale considering Y=15° (y=0.375 pu) and 32s of transition time corresponding to 8s transition at the reduced scale model.
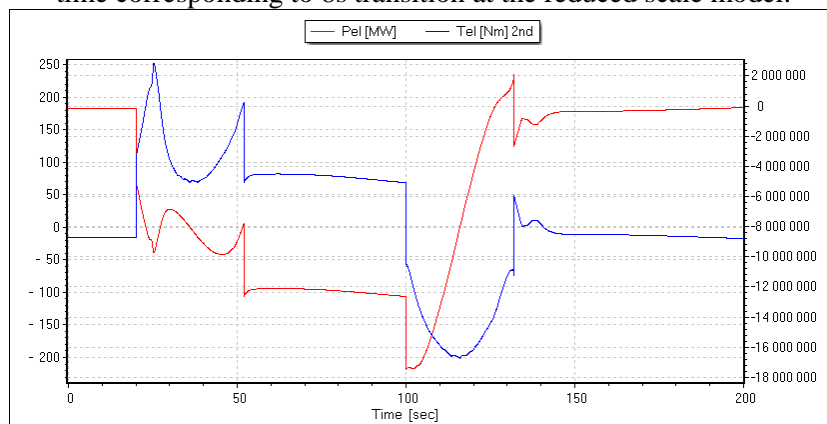


**Figure 15** Time evolution of the transient electromagnetic torque (Tel) and active power (Pel) of the motor-generator during the fast transition from pump to turbine and vice-versa at the prototype scale considering Y=15° (y=0.375 pu) and 32s of transition time corresponding to 8s transition at the reduced scale model, calculated using the simplified approach.

13

### 4.4. Comparison between hydromechanical and hydroelectric model

The simulation results of the fast transition from pump to turbine and vice versa in 32 s at the prototype scale, corresponding to 8s of transition at the reduced scale, and guide vane of Y=15° (y=0.375 pu) obtained with the simplified hydromechanical model are compared with the simulation results obtained with the fully detailed hydroelectric model for both hydraulic and electric quantities respectively in Figure 16. The very good agreement between both simulation results confirms the validity of simplified approach to estimate the electrical quantities in hydromechanical model using equations (3) and (4).
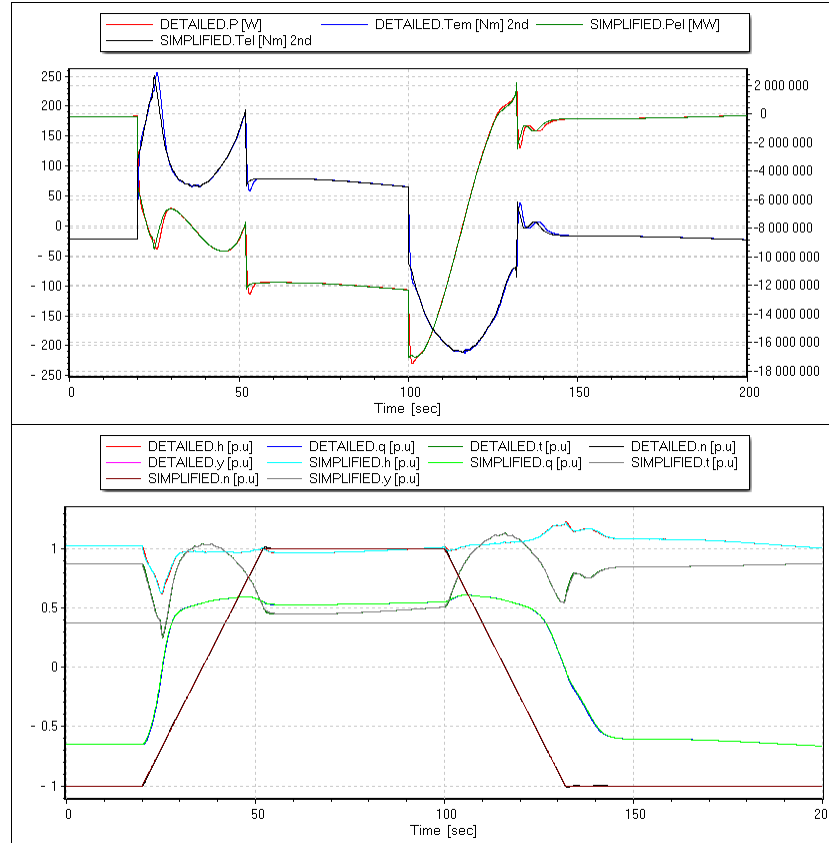


**Figure 16** Comparison of the time evolution of the transient electromagnetic torque and active power of the motor-generator (top) and hydraulic pump-turbine transient (bottom) during the fast transition from pump to turbine and vice-versa at the Prototype scale considering Y=15° (y=0.375 pu) and 32s of transition time corresponding to 8s transition at the reduced scale model, calculated using the simplified and detailed models.

### 4.5. Fast transition sequence optimization

As shown in the previous chapters, the fast transition from pump to turbine and vice versa may lead to extreme values of hydraulic and electrical quantities, evidencing the need and potential for fast transition optimization. Therefore, hydromechnical simulations have been performed at the prototype scale for the 4 different transition time considered at the reduced model scale of 4s, 8s, 12s and 20s corresponding respectively to 16s, 32s, 48s and 80s at the prototype scale. Therefore, the transition from turbine to pump and vice versa is simulated considering a guide vane opening sequence which starts from nominal opening in turbine mode, then is closed to Y=5° (y=0.125 pu) before the linear rotational speed transition from turbine to pump, after which the guide vane is reopen to optimal pump guide vane opening of Y=20° (y=0.5). For the transition from pump to turbine, the sequence is achieved in the opposite order.

Figure 17 presents the 4 different sequences considered in the optimization and the resulting simulation results of the time evolution of the pump-turbine net head, discharge, electromagnetic

torque and active power respectively presented in Figure 18, Figure 19, Figure 20 and Figure 21. The simulation results show that the net head rise occurring during the turbine to pump transition is not significantly affected by the transition time as the discharge reversal remains very sudden whatever the transition time, meaning that the optimization should probably combine rotational speed together with the guide vane opening sequence to minimize the overpressure in the spiral case and the low pressure in the draft tube. The analysis of electrical quantities shows that the transition from turbine to pump in 16s at the prototype scale would not be feasible as the active power reaches about 300 MW (1.42 pu) and electromagnetic torque of 1.8 times the nominal value, which would not be acceptable. So the minimum transition time from turbine to pump would be of 32s if this sequence is considered. However, it could be noticed that the transition from pump to turbine in 16s would not be problematic as the electrical quantities remains below nominal values. As a results, the transition from pump to turbine could be achieved two times faster than the transition from turbine to pump due to the gravity forces. The comparison between the admissible transition time and the mechanical time constant of 8.6 s, see Table 1, shows that for the power plant considered for this investigation and considering the proposed sequence, the transition from pump to turbine could be achieved approximately in twice the mechanical time constant, here 16s, while the transition from turbine to pump requires about 4 times the mechanical time constant. Of course, the present transition sequences could be further optimized to reduce the transitions time, but these simulation results provide a first order of magnitude of what could be achieved. It should be also noticed that in these simulations, the downstream surge tank water level remains within acceptable values, see Figure 22. However, the combination of transition sequences of the two units, and the risks of emergency shutdown during the transition sequence would have to be carefully addressed to ensure safe operation of the power plant when considering fast transition opportunity.
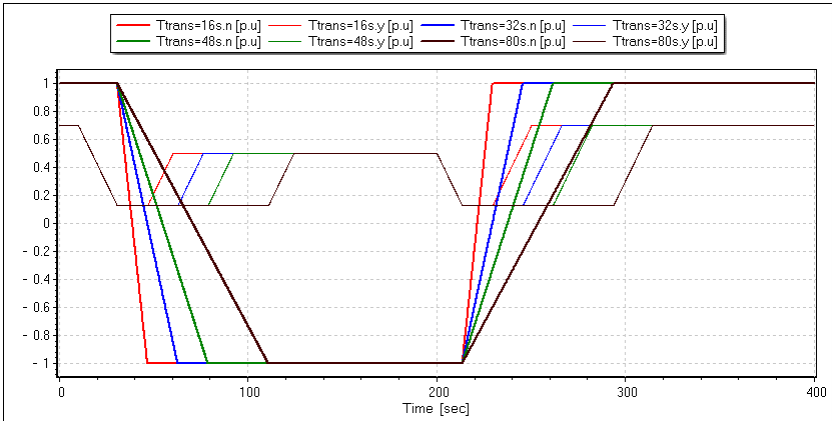


**Figure 17** Time evolution of guide vane opening and rotational speed sequences considered for fast transition sequence optimization considering 16s, 32, 48 s, and 80s of transition time and guide vane opening of Y=5° (y=0.125) during the transition.
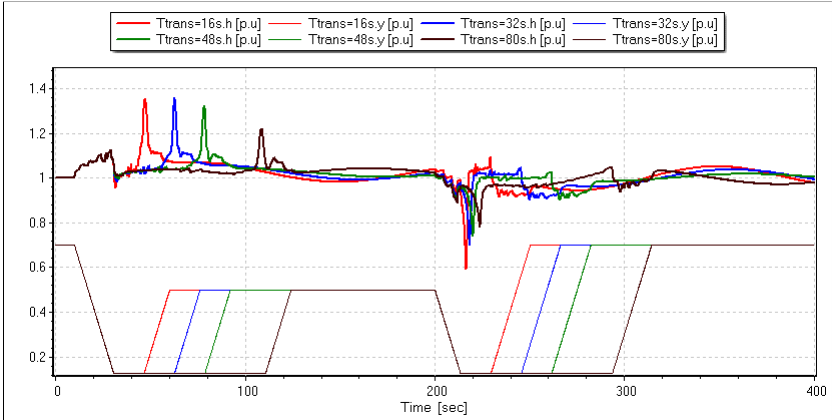


**Figure 18** Time evolution of the pump-turbine net head for fast transition sequences considering 16s, 32, 48 s, and 80s of transition time and guide vane opening of Y=5° (y=0.125) during the transition.
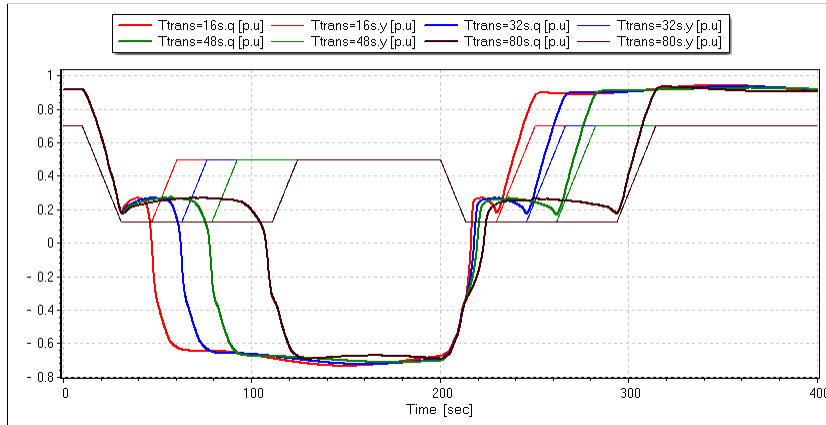
15

**Figure 19** Time evolution of the pump-turbine discharge for fast transition sequences considering 16s, 32, 48 s, and 80s of transition time and guide vane opening of Y=5° (y=0.125) during the transition.
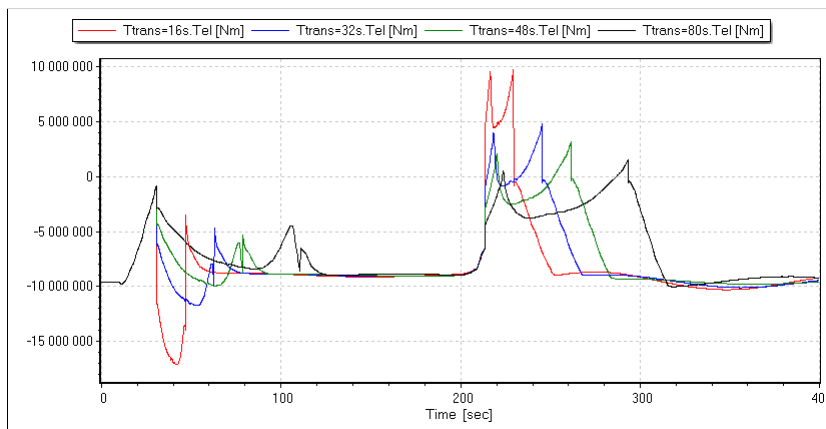


**Figure 20** Time evolution of the pump-turbine unit electromagnetic torque for fast transition sequences considering 16s, 32, 48 s, and 80s of transition time and guide vane opening of Y=5° (y=0.125) during the transition.



**Figure 21** Time evolution of the pump-turbine unit active power for fast transition sequences considering 16s, 32, 48 s, and 80s of transition time and guide vane opening of Y=5° (y=0.125) during the transition.

16

**Figure 22** Time evolution of the downstream surge tank water level for fast transition sequences considering 16s, 32, 48 s, and 80s of transition time and guide vane opening of Y=5° (y=0.125) during the transition.

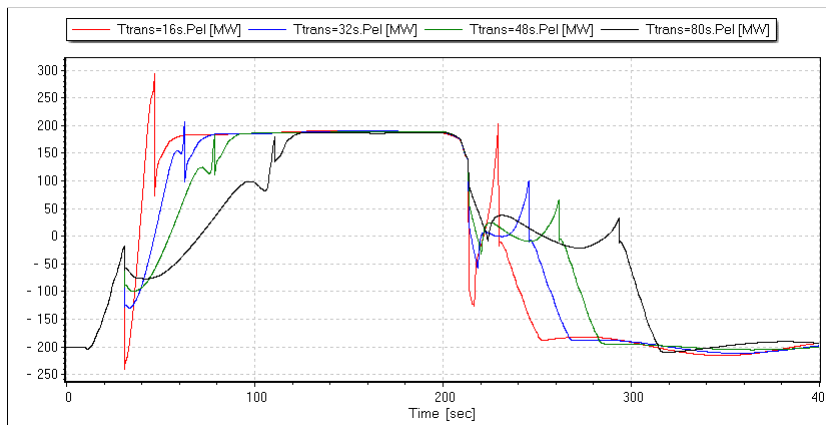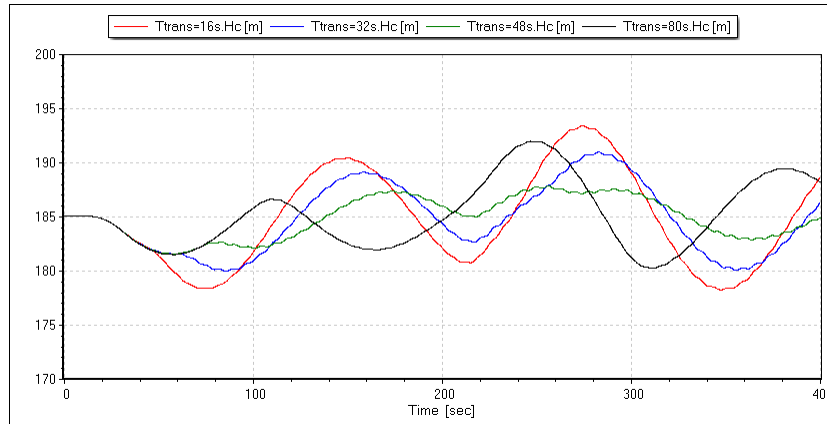## 5. Conclusions

The lean integration of intermittent New Renewable Energies requires additional power control services capabilities to ensure electrical grid stability. In this context, pumped storage power plants operating flexibility combined with recent development of power electronics enable to envisage new ancillary services such as fast active power injection or absorption and inertia emulation which can significantly contribute to secure power network operation. Full Size Frequency Converter synchronous machine unit offer new perspectives such as fast transition from pump to turbine and vice versa enabling to take full advantage of the entire pumped storage capacity from consumption to generation mode.

Such opportunity was deeply investigated in the framework of the European Research Project HYPERBOLE in order to assess the feasibility of fast mode transitions. Therefore, reduced scale model test investigations were carried out by means of both experimental and numerical approaches while the transposition to prototype was investigated by means of numerical simulation for an existing power plant which pump-turbine is quasi homologous to the reduced scale model. The main conclusions obtained from reduced scale model and prototype investigations are the following:

- Test rig facility was modified to carry out fast transition mode from pump to turbine and vice versa considering transition times varying from 4s to 20s at the reduced model scale corresponding to 16s to 80s transition time at the prototype scale for the considered test case;
- The comparison between measurements and 1 D numerical simulations at the reduced scale demonstrated to the ability of such 1 D numerical models to address fast transition mode from a system perspective; of course, consequences of the fast transition on the pump-turbine component lifetime have to addressed by means of detailed pump-turbine instrumentation and supported with 3D unsteady CFD analysis combined with FEM analysis of the component structure;
- Transposition of the transition time from model to prototype could be assessed considering Froude similitude where the transition time ratio between model and prototype is proportional to the square root of the runner reference diameter ratio;
- Simplified models for the motor-generator to be combined with hydromechanical model of the power plant have been proposed and validated against fully detailed models of FSFC motor-generator models to identify potentially excessive electromagnetic torque and active power during the transition sequence;
- Comparison between reduced scale model test and simulations and simulation results at prototype scale shows qualitatively similar results with sudden pump-turbine net head drop during the pump to turbine transition and net head sudden rise during turbine to pump transition resulting from the flow respective acceleration and deceleration; these net

head variations lead to spiral case and draft tube pressure variations to be carefully addressed;

- The investigation of influence of the transition time performed at the prototype scale by means of numerical simulation showed that as expected faster transition can be achieved from pump to turbine than from turbine to pump due to respective influence of the gravity forces for both transition;
- For the test case considered in the present study corresponding to a 2x210 MW existing pumped storage power plant, the transition time from pump to turbine was found to be about 2 times the mechanical time constant with 16 seconds of transition time while the transition from turbine to pump was found to be about 4 times the mechanical time constant with 32 seconds of transition time;
- The combination of fast transition sequences considering all power plant units and the risk of emergency shutdown during the transition sequences should be carefully addressed when considering the opportunity of fast transition mode;
- The system dynamic simulations presented here, combined with operational cost simulations represent appropriate tools for the optimization of pumped storage power plants ancillary services in view of a lean integration of intermittent New Renewable Energies.

Besides storage and substitution generation capabilities, pumped storage power plants can also significantly contribute to power network stability due to their considerable operating flexibility, and constant development of power electronics offers new opportunities enabling to increase further the attractiveness and competitiveness of hydropower.

## 6. Acknowledgments

## 7. Nomenclature

$A$: pipe cross section area [m$^2$]

$D_{ref}$: machine reference diameter [m]

$H$: net head [m]

$Q$: discharge [m$^3$/s]

$N$: rotational speed [min$^{-1}$]

$P$: power [W]

$T$: Torque [Nm]

$a$: pipe wave speed [m/s]

$h$: piezometric head $h=z+p/(\rho g)$ [m]

$g$: gravity [m/s$^2$]

$n$: rotating frequency [Hz]

$p$: static pressure [Pa]

$p$: pressure [Pa]

$t$: time [s]

$x$: position [m]

$y$: turbine guide vane opening [-]

$Z$: elevation above a datum [m]

$\omega$: rotational pulsation [rd/s]

$$n_{ED} = n \cdot D_{ref} \Big/ E^{0.5} \quad \text{speed factor} \ \text{[-]}$$

$$Q_{ED} = Q \Big/ (\mathrm{D}_{ref}{}^2 \cdot \mathrm{E}^{0.5}) \quad \text{discharge factor [-]}$$

$$T_{ED} = T \Big/ (\rho \cdot \mathrm{D}_{ref}{}^3 \cdot \mathrm{E}) \quad \text{torque factor [-]}$$

$$n_{QE} = nQ^{0.5} \Big/ E^{0.75} \quad \text{specific speed [-]}$$

$$N_{11} = N \cdot D_{ref} \Big/ H^{0.5} \quad \text{unit speed factor} \ \text{[rpm}\cdot\text{m}^{0.5}\text{]}$$

$$Q_{11} = Q \Big/ (\mathrm{D}_{ref}{}^2 \cdot H^{0.5}) \quad \text{unit discharge factor [m}^{0.5}\text{/s]}$$

$$T_{11} = T \Big/ (\mathrm{D}_{ref}{}^3 \cdot H) \quad \text{unit torque factor [N/m}^3\text{]}$$

## 8. References

[1]     Antheaume, S., Darona, G., Houdeline, J.-B., Labrecque, Y., Laurier, P., "Comparison of Pump Storage retrofit and upgrade to variable speed through two recent case studies in Europe", Proceedings of Hydrovision Conference 2014, July 22-25, 2014, Nashville, TN, USA.

[2]     Aubert, S., Linder, S., Steimer P. K., Hillberg, C., "Variable speed pumped storage with converter-fed synchronous machines (CFSM) – a high value in grids with high penetration of wind and solar generation", Proceedings of HYDRO 2014, in Cernobbio, Italy, paper 13b.02.

[3]     Canay, I. M., "Extended synchronous machine model for calculation of transient processes and stability", Electric machines and Electromechanics, vol. 1, pp. 137-150, 1977.

[4]     Canay, I. M., "Physical significance of sub-subtransient quantities in dynamic behaviour of synchronous machines", Electric Power Applications, IEE Proceedings B  (Volume:135 , Issue: 6), pp. 334-340, Nov. 1988.

[5]     Fisher, R. K., et al., "A Comparison of Advanced Pumped Storage Equipment Drivers in the US and Europe", Louisville, USA, Hydrovision 2012.

[6]     Grotenburg, K., Koch, F., Erlich, I., Bachmann, U., "Modeling and Dynamic Simulation of Variable Speed Pump Storage Unit Incorporated into the German Electric Power System", EPE 2001, Graz, Austria, 2001.

[7]     Hildinger T., Kodding, L., "Modern design for variable speed motor-generators-asynchronous (DFIM) and synchronous (SMFI) electric machinery options for pumped storage powerplants", Innsbruck, Hydro 2013.

[8]     Hell J., Egretzberger M., Lechner A., Schürhuber R., Vaillant Y., "Full size converter solutions for pumped storage plants – a promising new technology", Hydro2012, Euskalduna Congress Centre Bilbao, Spain, 29-31 October 2012.

[9]     Hell J., Egretzberger M., Lechner A., "Grid frequency response – contribution of hydro power for grid stabilization", Proceedings of Hydro2014, Cernobbio, Italy, paper 25.04.

[10]    Kawkabani, B., Nicolet, C., Schwery, A., "Modeling and control of large salient-pole synchronous hydro generators and stability issues in isolated production mode", 2013 IEEE Workshop on  Electrical Machines Design Control and Diagnosis (WEMDCD), Pages 148 - 157.

[11]    Kopf, E., Brausewetter, S., Giese, M., Moser, F., "Optimized control strategies for variable speed machines," In Proceeding of the 22nd IAHR Symposium on Hydraulic Machinery and Systems, Stockholm, Sweden, June –July 2004.

[12]    Koutnik, J., Bruns, M., Meier, L., Nicolet, C., Pumped Storage - Grid Requirements For Behavior of Large Motorgenerators and Confirmation Of Compliance Through Simulation, Proceedings of HydroVision International, 19-22 July 2011, Sacramento, CA, USA, Session: Pumped Storage Design, Technology and Operation, pp. 1-11.

[13]    Koutnik, J., Foust, J., Nicolet, C., Saiju, R., Kawkabani, B., Pump-Storage Integration with Renewables – Meeting the Needs Using Various Concepts, Proceedings of HydroVision International, 27-30 July 2010, Charlotte, NC, USA, Session: Pumped-Storage Market Trends and Strategies, paper 5, pp. 1-12.

[14]    Koritarov, V., "Modeling and Analysis of Value of Pumped Storage Hydro", NHA Annual Conference 2013, Washington, DC, USA. http://www.dis.anl.gov/psh

[15]   Kuwabara, T., Shibuya, A., Furuta, H., Kita, E., Mitsuhashi, K., "Design and Dynamic Response Characteristics of 400 MW Adjustable Speed Pumped Storage Unit for Ohkawachi Power Station", IEEE Transactions on Energy Conversion, vol. 11, issue 2, pp. 376-384, June 1996.

[16]   Kunz, T., Schwery, A., Guillaume, R., Teller, O., "Variable speed pumped storage plants: Project execution and development towards new operation", Proceedings of Hydro2015, Bordeaux, France, paper 26.01.

[17]   Martins, N., et al., "The integration of large amounts of renewable energy in the Portuguese Power System", SHF : «Pumped storage Powerplants», Lyon, nov. 2011.

[18]   Nicolet, C., "Hydroacoustic modeling and numerical simulation of unsteady operation of hydroelectric systems", Thesis EPFL n° 3751, 2007, (http://library.epfl.ch/theses/?nr=3751).

[19]   Nicolet, C., Greiveldinger, B., Hérou, J.-J., Kawkabani, B., Allenbach, P., Simond, J.-J., Avellan, F**.,** "High Order Modeling of Hydraulic Power Plant in Islanded Power Network", IEEE Transactions on Power Systems, Vol. 22, Number 4, November 2007, pp.: 1870-1881.

[20]   Nicolet, C., Pannatier, Y., Kawkabani, B., Schwery, A., Avellan, F., Simond, J.-J., "Benefits of Variable Speed Pumped Storage Units in Mixed Islanded Power Network during Transient Operation", Proceedings of HYDRO 2009, in Lyon, France.

[21]   Pannatier, Y., Nicolet, C., Kawkabani, B., Simond, J.-J., Allenbach, Ph., "Dynamic Behavior of a 2 Variable Speed Pump-Turbine Power Plant", ICEM 2008, XVIII International Conference on Electrical Machines, Vilamoura, Portugal, September 2008.

[22]   Pannatier, Y., Kawkabani, B., Nicolet, C., Simond, J.-J., Schwery, A., Allenbach, P., Investigation of control strategies for variable speed pump-turbine units by using a simplified model of the converters,  IEEE Transactions on Industrial Electronics, Volume: 57, Issue: 9, 2010, pp: 3039-3049.

[23]   Ruchonnet, N., Braun, O., "Reduced scale model test of pump-turbine transition". 6th IAHR International Meeting of the Workgroup on Cavitation and Dynamic Problems in Hydraulic Machinery and Systems, Ljubljana. 2015.

[24]   Sapin, A., "Logiciel modulaire pour la simulation et l'étude des systèmes d'entraînement et des réseaux électriques", Thesis EPFL n° 1346, 1995, (http://library.epfl.ch/theses/?nr=1346).

[25]   Schlunegger, H., Thöni, A., "100MW full-site converter in the Grimsel 2 pumped-storage plant", Innsbruck, Hydro 2013.

[26]   Schwery, A., Kunz, T., Gökhan, S., "Adjustable speed pumped storage plants – Innovation challenges and feedback of experience from recent projects", Hydrovision International, Louisville, KY, USA, 2012.

[27]   Schrepler, R., Schöner, T., Aschenbrenner, T., "Hydraulic application aspects on variable speed pump-turbines", Proceedings of HYDRO 2014, October 13-15, 2014, in Cernobbio, Italy, Paper 13d.08.

[28]   Spitzer, F., Penninger, G., "Pumped storage power plants – Different solutions for improved Ancillary services through rapid response to power needs", Hydrovision 2008, Sacramento, USA, July 14-18, 2008, paper 180.

[29]   Stens, C., Riedelbauch, S., "CFD simulation of the flow through a pump turbine during a fast transition from pump to generating mode". 6th IAHR International Meeting of the Workgroup on Cavitation and Dynamic Problems in Hydraulic Machinery and Systems, Ljubljana. 2015.

[30]   U.S. Energy Information Administration, "International Energy Outlook (IEO) 2013", DOE/EIA-0484 (2013), July 2013. http://205.254.135.7/forecasts/ieo/pdf/0484(2013).pdf

[31]   Wylie, E. B. & Streeter, V.L., "Fluid transients in systems". Prentice Hall, Englewood Cliffs, N.J, 1993.

[32]    https://hyperbole.epfl.ch

## The Authors

**Dr Christophe NICOLET** graduated from the Ecole polytechnique fédérale de Lausanne, EPFL, in Switzerland, and received his Master degree in Mechanical Engineering in 2001. He obtained his PhD in 2007 from the same institution in the Laboratory for Hydraulic Machines. Since, he is managing director and principal consultant of Power Vision Engineering Sàrl in Ecublens, Switzerland, a company active in the field of optimization of hydropower operation. He is also lecturer at EPFL in the field of "Transient Flow in Systems".

**Dr Olivier BRAUN** graduated from the TU Berlin, in Germany and received his Master degree in Mechanical Engineering in 2001. Between 2001 and 2003 he worked for ANSYS Germany as customer support engineer for numerical flow simulation. He obtained his PhD in 2009 from EPFL. Since 2009 he joined Andritz Hydro SA, Switzerland. He is currently head of the Turbine Physics group.

**Dr Nicolas RUCHONNET** received his Master degree in Mechanical Engineering in 2006 and his PhD in 2010 from the Ecole polytechnique fédérale de Lausanne, EPFL. Since 2011, he is working for Andritz Hydro SA, Switzerland. From 2011 to 2014, he worked as development Engineer in the Mechanical Analysis group in Zurich. In 2014 he joined the Turbine Physics group in Vevey.

**Dr Antoine BEGUIN** graduated from the Ecole polytechnique fédérale de Lausanne, EPFL, in Switzerland, and received his Master degree in Electrical Engineering in 2006. He obtained his PhD in 2011 from the same institution in the Laboratory for Power Electronics in the field of Poly-phased Matrix Converter development and optimisation. Since, he is working with Power Vision Engineering Sàrl in Ecublens, Switzerland.

**Mr. Johann HELL** is a member of the Electrical Power System division of ANDRITZ HYDRO, Vienna, Austria. Graduated at the Vienna University of Technology he works about 15 years in the field of Sales and R&D for variable speed drives and frequency converters. Since 1999 he was project engineer for generator tenders. Since 2008 he is responsible for Electrical Power Engineering in ANDRITZ HYDRO. Since 2013 he is Principal Engineer for system simulation and also responsible for R&D of Electrical Power Systems.

**Prof. François AVELLAN** graduated in Hydraulic Engineering from INPG, Ecole Nationale Supérieure d'Hydraulique, Grenoble France, in 1977 and, in 1980, got his doctoral degree in engineering from University of Aix-Marseille II, France. Research associate at EPFL in 1980, he is director of the Laboratory for Hydraulic Machines since 1994 and was appointed Ordinary Professor in 2003. From 2002 to 2012, Prof. F. Avellan was Chair of the IAHR Committee on Hydraulic Machinery and Systems.